Systems Chemistry across Multiple Length Scales: Macroscopic Flow via Dissipative Co-Assemblies Featuring Transient Amides

Kai Liu, Alex W. P. Blokhuis, Sietse J. Dijt, Shana Hamed, Armin Kiani, Bartosz M. Matysiak and Sijbren Otto*

Centre for Systems Chemistry, Stratingh Institute
University of Groningen
Nijenborgh 4, 9747 AG, Groningen (the Netherlands)
E-mail: s.otto@rug.nl

Abstract: Fueled chemical systems have considerable functional potential that is still largely unexplored. Here, we report a new approach to transient amide bond formation and use it to harness chemical energy and convert it to mechanical motion by integrating dissipative self-assembly and the Marangoni effect in a source-sink system. Droplets are formed through dissipative self-assembly following the reaction of octylamine with 2,3-dimethylmaleic anhydride. The resulting amides are hydrolytically labile making the droplets transient, which allows them to act as a source of octylamine. A sink for octylamine was created by placing a drop of oleic acid on the air-water interface. This source – sink system sets up a gradient in surface tension, which gives rise to a macroscopic Marangoni flow that can transport the droplets in solution with tunable speed. Carbodiimides can fuel this motion by converting diacid waste back to anhydride. This study shows how fueling at the molecular level can, via assembly at the supramolecular level, lead to liquid flow at the macroscopic level.

Keywords: self-assembly • energy dissipation • active matter • droplets • motion • Marangoni effect

Introduction

Life is a far-from-equilibrium system where the maintenance of structures and performance of functions are powered by consumption of energy[1]. Energy stored in small molecules can be converted to work on a much larger length scale: for example, microtubules use the energy of guanosine triphosphate to separate chromosomes through a mechanical force[2]. In recent years chemists are becoming increasingly interested in synthetic non-equilibrium systems to better understand non-equilibrium processes in life and to design systems with specific functions[3]. This interest has given rise to the field of dissipative self-assembly[4-9], which has focused on transient structures and associated properties with programmable lifetimes[10-19]. Structures in states that rely on a continuous input of energy bridge chemical and biological self-assembly[20], however, they are incompletely understood and remain difficult to design[21]. It is challenging to channel energy in a productive way and avoid direct dissipation into heat. In addition, relatively few chemical reactions are available that readily allow for a fueled bond making and breaking cycle. It is also difficult to design systems that go beyond assembly and exhibit more advanced emergent properties[22], such as structural change[23,24] or oscillations[25,26]. Coupling dissipative self-assembly with mechanical processes could be a promising path toward new emergent behavior[9].

Chemical energy can drive motion to give rise to dynamic patterns, and perform work in (bio)molecular motors[27,28] and in active matter[29]. Energy stored in molecules can directly be converted to mechanical motion through chemical reactions in chemically powered motors[30]. Concentration gradients are also widely applied for powering motion, such as diffusiophoretic transport at the fluid-solid interface[31] and Marangoni effects that displace a liquid drop on solid surfaces[32] or in liquid[33,34] or move objects at an air/liquid interface[35-37]. When a surface tension gradient is developed by

a concentration gradient, Marangoni convection will transport mass to areas of higher surface tension[38]. Such Marangoni effects can be magnified by depletion of surfactant through crystallization[39], supramolecular interaction[40], or a light-induced chemical reaction to increase the gradient in surface tension[41]. Most studies focus on the conversion of free energy into motion without involving structural changes to the molecules in the system. We reasoned that it should be possible to broaden the scope of Marangoni convection systems by chemical fueling. This approach would unify dissipative self-assembly and Marangoni motion within a self-organized network. Dissipative chemistry may offer a feasible method to control Marangoni convection by tuning and sustaining its underlying driving force.

Herein, we introduce a new approach to dissipative amide chemistry to produce transient droplets based on chemically fueled self-assembly. These droplets act as a source of surfactant to produce Marangoni convection in a source-sink system. The droplets are formed from the reaction of 2,3-dimethylmaleic anhydride (**1a**) with octylamine (**2**) and followed by co-assembly of amphiphilic maleamic acid (**3a**; reaction product) and remaining (or re-formed) octylamine (Figure 1a). The amide bond in the maleamic acid is hydrolysable, which makes the droplets transient and causes the continuous release of octylamine. The amide-based droplets are regenerable by adding a chemical fuel (i.e. anhydride or carbodiimide reagent) (Figure 1a). These droplets are transported towards an oleic acid droplet placed on the air/water interface, that acts as a sink for octylamine. Transport is driven by Marangoni fluid convection (Figure 1b,c). Thus, the dynamic instability of the amide-based droplets is converted into a gradient of octylamine surfactant at the air-water interface, which leads to a surface tension gradient that gives rise to a Marangoni instability. This study couples dissipative self-assembly to macroscopic fluid flows.

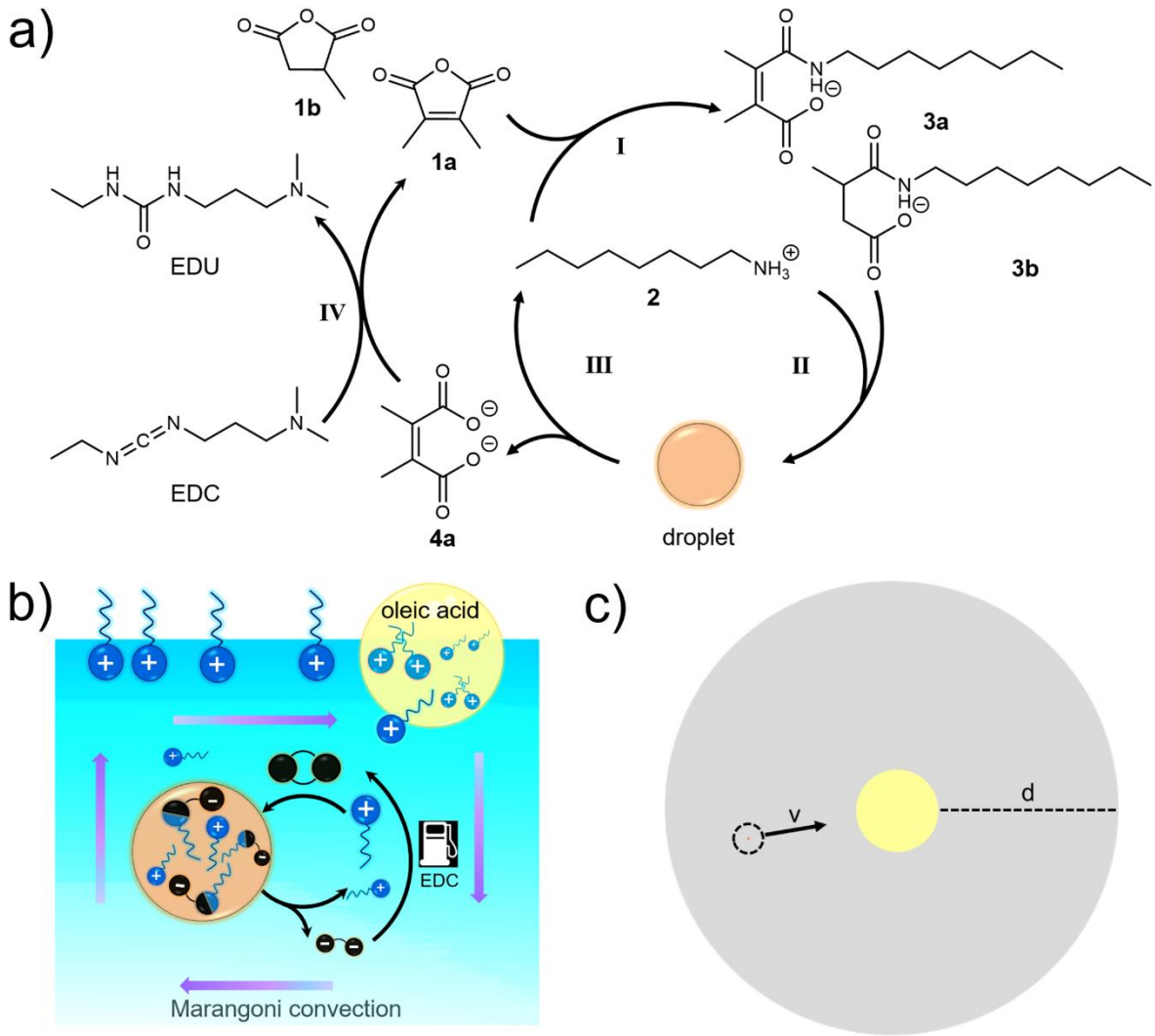

Figure 1. a) Dissipative self-assembly of amide-based droplets. Droplets are formed after a chemical reaction (I) followed by co-assembly of amide product **3** and amine **2** (II). Amide hydrolysis leads to the disintegration of the droplets (III). Upon the addition of N-(3-dimethylaminopropyl)-N'-ethylcarbodiimide (EDC), diacid **4** is converted back into cyclic anhydride **1** (IV), which can enter into another reaction/assembly/hydrolysis/disintegration cycle. b) EDC-fueled Marangoni convection in a source-sink system (side view), where an oleic acid droplet (top right) captures the octylamine released from the amide-based droplets to generate a concentration gradient of surfactant at the air/water interface that is sustained as long as the amine continues to be released. c) Schematic presentation (top view) of the transport of an amide-based droplet (in the dashed circle) towards the oleic acid (yellow

area in the middle). The gray circle indicates the area where movement occurs, where the length scale (d ≈ 2 mm, determined by microscopic observation) is at least a thousand times larger than the size of an amide-based droplet.

Dissipative co-assembly of coacervate-like droplets

Dispersing octylamine (**2**, 30 mM) in an aqueous solution containing sodium borate (50 mM, pH 8.2), gave rise to an almost transparent mixture (Figure S2). However, upon adding 2,3-dimethylmaleic anhydride (**1a**, 30 mM) followed by shaking by hand for ~60 s, the turbidity of the above solution increased substantially (Figure S2), resulting from the formation of microdroplets (Figure S3). Analysis by cryogenic transmission electron microscopy (cryo-TEM) during the early stages of growth shows a uniform structure inside the droplets (Figure 2a). These droplets were found to coalesce (Figure S3), suggesting that also the larger droplets are similarly uniform. The thus formed droplets have a size of ~2.5 μm, which is much larger than the droplets formed upon dispersing octylamine (Figure 2b). ^{1}H-NMR analysis (Figure S4a) confirmed that in the resulting samples amide bonds had formed, which result from the condensation between amine and anhydride[42]. MS analysis confirmed that **3a** is the main product (Figure S5).

An apparent critical concentration of **3a** for the formation of droplets in the mixture made from **1a** and **2** is about 7 mM (Figure S10). However, when pure **3a** (30 mM) was directly dissolved in sodium borate (50 mM, pH 8.2) solution, no droplet formation was observed, and droplets only appeared after adding **2** (Figure 2c and Figure S12). These results suggest that the liquid-liquid phase separation occurs from the spontaneous co-assembly of **3a** and **2**, reminiscent of complex coacervate formation[43]. The zeta potentials of the pure octylamine and amide droplets are +15 mV and -98 mV, respectively (Figure 2d), indicating that the surface of the amide-based droplets mainly

consists of carboxylate groups which outnumber the positive charges from the amine groups. The amide-based droplets are capable of taking up negatively charged calcein (Figure 3e) and positively charged acriflavine (Figure S13), confirming the catanionic nature of these droplets[44].

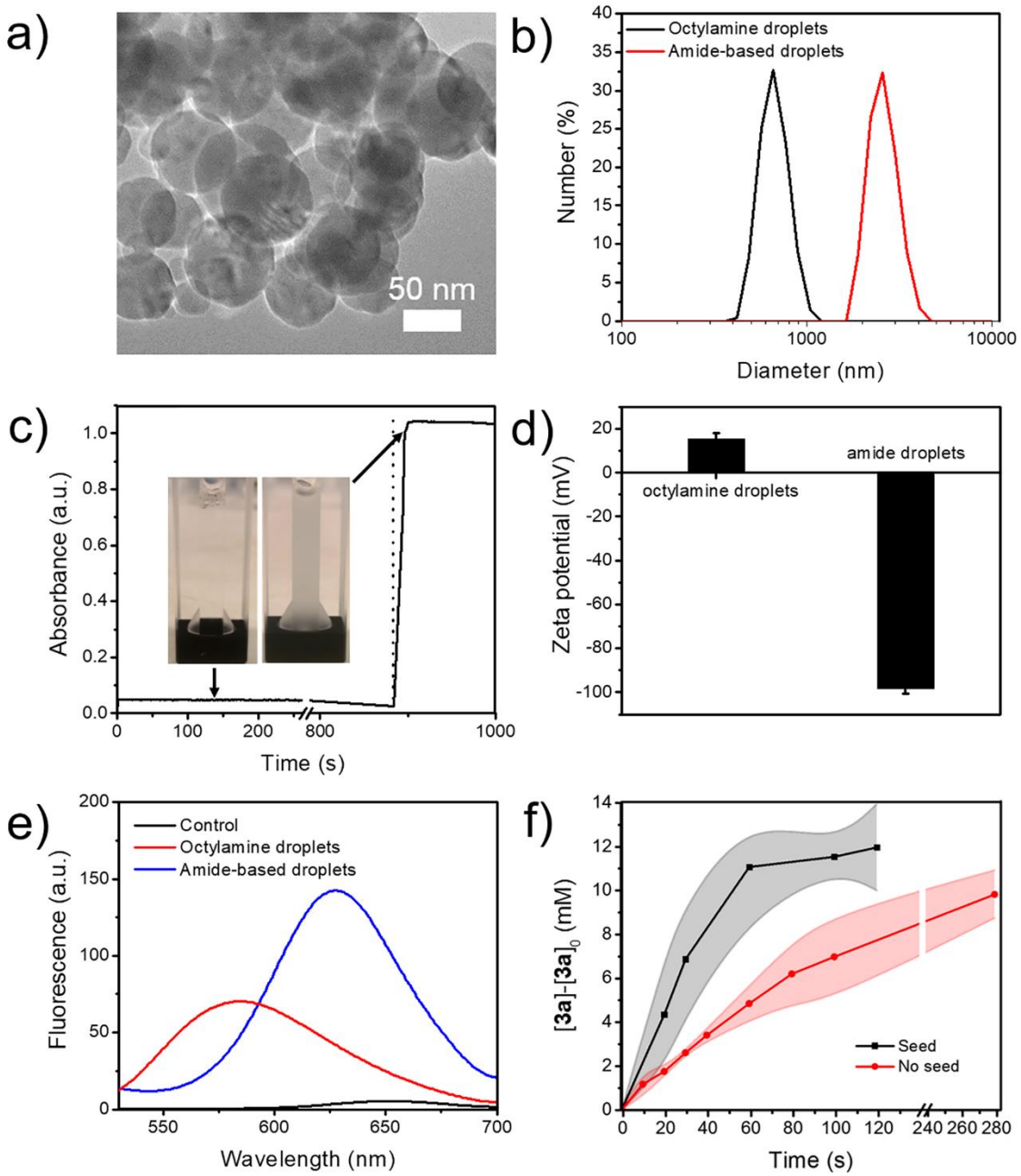

Figure 2. a) Cryo-TEM image capturing the early phase of amide-based droplet formation upon mixing **2** (30 mM) with **1a** (30 mM) in an aqueous solution containing

sodium borate (50 mM, pH 8.2). b) Size distribution of the amide-based droplets in (a) upon longer incubation and octylamine droplets prepared by dispersing **2** (30 mM) in an aqueous solution containing sodium borate (50 mM, pH 8.2). c) Change of the turbidity of the **3a** (30 mM) solution containing sodium borate (50 mM, pH 8.2) before and after adding **2** (6.0 mM) as indicated by the dashed line. The insets are photos of the corresponding solutions. d) Zeta potential of the amide-based droplets in (a). Error bars represent standard deviations (*n*=3). e) Fluorescence of Nile red (1.0 μM) in the presence of amide-based or octylamine droplets in (b). Nile red in the above aqueous solution was used as control. f) Production of **3a** from **2** (12 mM) and **1a** (12.7 mM) in an aqueous solution containing sodium borate (50 mM, pH 8.2) in the absence (gray line) or presence (black line) of pre-prepared amide-based droplets (prepared from **2** (30 mM) and **1a** (30 mM)). The concentration was measured by UPLC after diluting the samples in DMF immediately prior to analysis. Shaded areas show the standard deviation (*n*=3).

When a hydrophobic probe (Nile red) was added to the amide-based droplets, its fluorescence maximum shifted to a lower wavelength (Figure 2e) compared to Nile red in water, indicative of a relatively hydrophobic microenvironment (albeit less hydrophobic than that provided by octylamine), indicating that the amide droplets also bind hydrophobic substrates.

The rate of formation of **3a** was enhanced upon addition of pre-prepared amide droplets (Figure 2f). This behavior is reminiscent of an autocatalytic process. We speculate that the amide-based droplets enhance the dissolution of **1a** to promote the condensation reaction, with concomitant droplet growth, similar to the phenomenon of autopoiesis[45].

The amide bond in **3a** is labile and readily hydrolyses to release **2** (Figure S4b). Such rapid hydrolysis is unusual for amide bonds and has been attributed to the

neighboring carboxylic acid catalyzing the hydrolysis through anchimeric assistance[46]. This effect is most pronounced for amides derived from 2,3-dimethylmaleic anhydride.

Surprisingly, the turbidity of the mixture made from **2** and **1a** first increased, then showed a rapid decrease, then increased again, and finally vanished permanently (Figure 3a). The generated **3a** does not follow the same trend, but only showed a buildup followed by a decrease (Figure 3b). This behavior can be explained considering that amide-based droplets form by co-assembly of amide and amine. Initially droplets form as the amide concentration increases, but only as long as there is still amine present as well. When amide formation progresses further, amine becomes depleted and the droplets disappear. They re-appear as amide starts to hydrolyze, generating, once again, a mixture of amine and amide. Once all amide has hydrolyzed, the droplet finally vanish for good. The formation/destruction/formation/destruction dynamics of the droplets is mirrored in the way droplet size changes with time (Figure 3c). The timescale of the dynamics was found to depend on the concentration of **1a**: when this concentration was increased from 35 mM to 45 mM, the timescale was reduced by a factor of about 4 (Figure 3b). We ascribe the strong sensitivity to concentration to the diacid that is generated upon hydrolysis of **3a**; a more acidic medium enhances the rate of hydrolysis[42]. In conclusion: due to the antergic relationship between **3a** and **2**, the droplets show a quite unusual non-linear behavior, which sets them apart from most other fueled droplets[17-19].

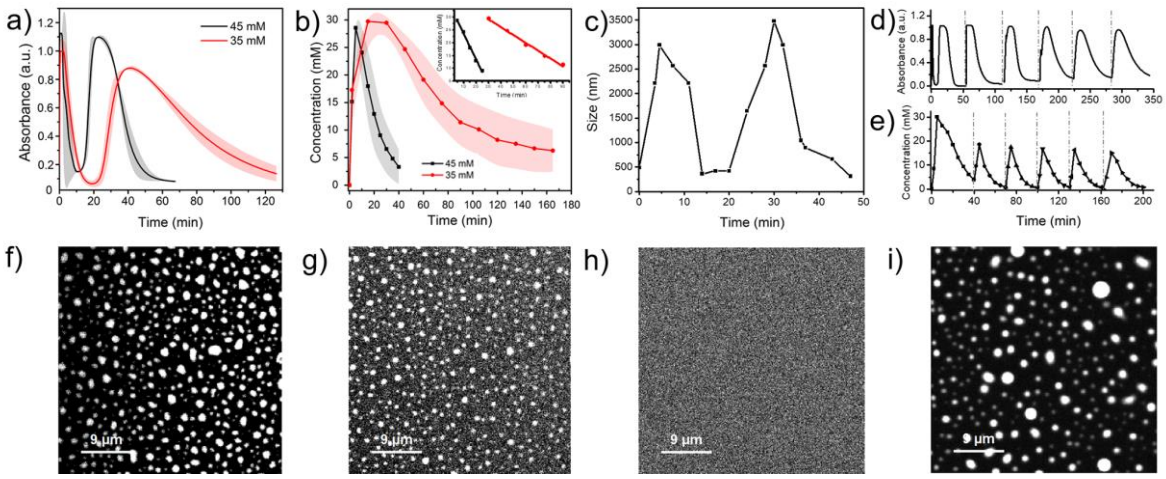

Figure 3. Time-dependent change of the (a) turbidity (b) concentration of **3a** determined by UPLC analysis in a mixture of **2** (30 mM) and **1a** (35 or 45 mM) in an aqueous solution containing sodium borate buffer (50 mM, pH 8.2). The inset in (b) shows the data points used to estimate the difference in the rate of hydrolysis of **3a** at different concentrations of **1a.** Shaded areas show the standard deviation (*n*=2 in panel a; *n*=3 in panel b). c) Time-dependent change of the size of the amide-based droplets prepared by mixing **2** (30 mM) and **1a** (45 mM) in an aqueous solution containing sodium borate (50 mM, pH 8.2). Time-dependent change of the (d) turbidity and (e) concentration of **3a** in the mixture prepared by mixing **2** (30 mM) and **1a** (45 mM) in an aqueous solution containing sodium borate (50 mM, pH 8.2). The arrows indicate the time points when EDC-HCl (60 mM) was added. Shaded areas in (a), (b), and (d) show the standard deviation. Confocal micrographs of amide droplets prepared as for (c) but now also in the presence of calcein (5.0 µM; added as disodium salt) after incubation for (f) 15 min, (g) 30 min, and (h) 40 min. i) Confocal micrograph of (h) after adding EDC (30 mM) and incubating for 5 min.

The amide-based droplets can be regenerated after the addition of the second batch of **1a** (Figure S15). Alternatively, in order to re-cycle all the structural components of the system, EDC can be used to regenerate the anhydride from the diacid product[47]. When EDC hydrochloride (EDC-HCl, 60 mM; this worked better than the “free” EDC allowing for more cycles before fatigue sets in; see Figure S18) was added to the clear

solution (pH ~5.0) where the amide-based droplets were no longer detectable, the solution became turbid again due to the renewed formation of droplets (Figure 3d, Figure S16). NMR analysis showed that EDC can induce the formation of amide by converting diacid **4a** back to anhydride **1a** which then reacts with **2** (Figure S17a). The double pulse that was observed in Figure 3a did not occur upon EDC fueling, as the rate at which EDC produces **1a** is not fast enough to deplete all octylamine before it is regenerated through hydrolysis of **3a**. As expected, after the EDC had been consumed, the turbidity decreases again (Figure 3d), due to the hydrolysis of the amide (Figure S17b and Figure 3e). When a second aliquot of EDC was added to the system (pH ~6.0), **3a** was again formed efficiently and droplets re-appeared. This EDC-fueled regeneration can be repeated at least 5 times (Figure 3d,e).

Guest molecules can be sequestered by the amide-based droplets upon EDC-fueled transient self-assembly, as evident from the confocal microscopy images using calcein as a guest (Figure 3f-i). Upon the disintegration of the droplets calcein is released into the medium (Figure 3h), but taken up again in the new droplets that form upon adding another aliquot of EDC (Figure 3i).

Droplet transport by chemically fueled macroscopic flow

A source-sink approach has been widely used to construct interactive droplet systems[48,49]. Having established that the amide-based droplets form transiently and constitute a source of amine surfactant **2** we proceeded by adding a localized sink for this surfactant, by placing a large droplet of oleic acid (0.2 µL) on the surface of the sample. In the resulting source-sink system (prepared using 35 mM **1a**), the amide-based droplets close to the surface started to move toward the oleic acid droplet, while the droplets further away from the surface below the focal plane were moving in the

opposite direction (Video S1), suggesting convective hydrodynamic flow. The initial average speed at which the amide-based droplets travelled was of the order of 700 μm s^{-1} over a length scale of several millimeters. Motion lasted for about 30 min.

In order to probe the importance of the labile character of amide **3a** for the observed behavior, we performed control experiments using droplets prepared by mixing methylsuccinic anhydride (**1b**) and **2** (Figure S19). These droplets contained amide **3b**, which is a non-hydrolysable analogue of **3a**. In the presence of an oleic acid droplet, they induce motion with a considerably slower average speed of ~100 μm s^{-1}, and for a considerably shorter period of time (halting after ~20 s; Video S2), compared to the droplets based on the hydrolysable amide. These results imply that the motion is fueled by the amide hydrolysis process.

The observed chemically fueled motion most likely occurs through the following mechanism: octylamine **2** (protonated) is a surfactant and will assemble at the air-water interface so that its nonpolar alkyl chains are removed from the aqueous environment. The adsorption of **2** at the water surface reduces the surface tension (see model analysis in the SI). The amide droplets are capable of releasing **2** during hydrolysis, which would normally lead to formation of a uniform monolayer at the air/water interface. However, when a droplet of oleic acid is added to the surface, it will act as a sink, sequestering **2**. Therefore, the surface concentration of **2** close to the oleic acid droplet will be lower than further away, resulting in surface tension gradient (the surface tension will decrease radially with the distance from the oleic acid droplet). Such surface tension gradients are well known to cause convective fluid flow (Marangoni flow) from sites with a low surface tension to sites with a high surface tension[38]. This results in the flow of the amide droplets near the air-water interface towards the oleic acid on the water surface. In order to balance the fluid level across

the sample a counter-current will develop further away from the surface, so that the system will develop a convection cell, analogous to Rayleigh–Bénard convection where order emerges from flow driven by a temperature gradient[50].

The validity of this mechanism was supported by the agreement of experimental observations with the qualitative features (recirculation; Figure 4a) obtained using a computational model of the proposed convection mechanism. The model includes surfactant production from a source and sequestration by a sink (for details see SI) to produce a surface tension gradient that furnished a driving force. Higher rates of surfactant production and sequestration leads to an increased gradient in surface tension, which, in turn, leads to an increased flow speed (Figure S20). Similar tendencies were also observed in the experimental systems. When amide droplets with higher (prepared in 45 mM **1a** instead of 30 mM) or lower (prepared at an elevated pH of 8.8 instead of 8.2) hydrolysis rate were used (Figure S20), the average speed increased (Video S3) or decreased (Video S4), respectively (Figure 4b).

Further support for the role of oleic acid as a sink comes from the observation that the speed of motion decreased as the oleic acid became saturated with **2** (Video S5, the same sample as in Video S1). However, it recovered when new oleic acid was added (Video S6). Support for the role of the amide as a source comes from the observation that the Marangoni flow stops when the amides are all hydrolyzed, even in the presence of fresh oleic acid. No motion of polystyrene microspheres trackers was observed under these conditions (Video S7). A control experiment was performed to show that these microspheres are in principle suitable to monitor the flow in these systems: when a droplet of oleic acid was placed on an aqueous solution containing **2** and polystyrene microspheres, the latter are initially transported with an average speed of ~300 μm s^{-1}(Video S8), but motion stops already after ~30 s (Video S9). In this case,

the initially transparent oleic acid droplet quickly became cloudy, most likely due to the capture of a large amount of **2** from the surrounding solution. The concentration gradient of **2** would thus fade fast. The relatively gradual release of **2** from the amide droplets is an efficient way to sustain the concentration gradient to power the Marangoni flow.

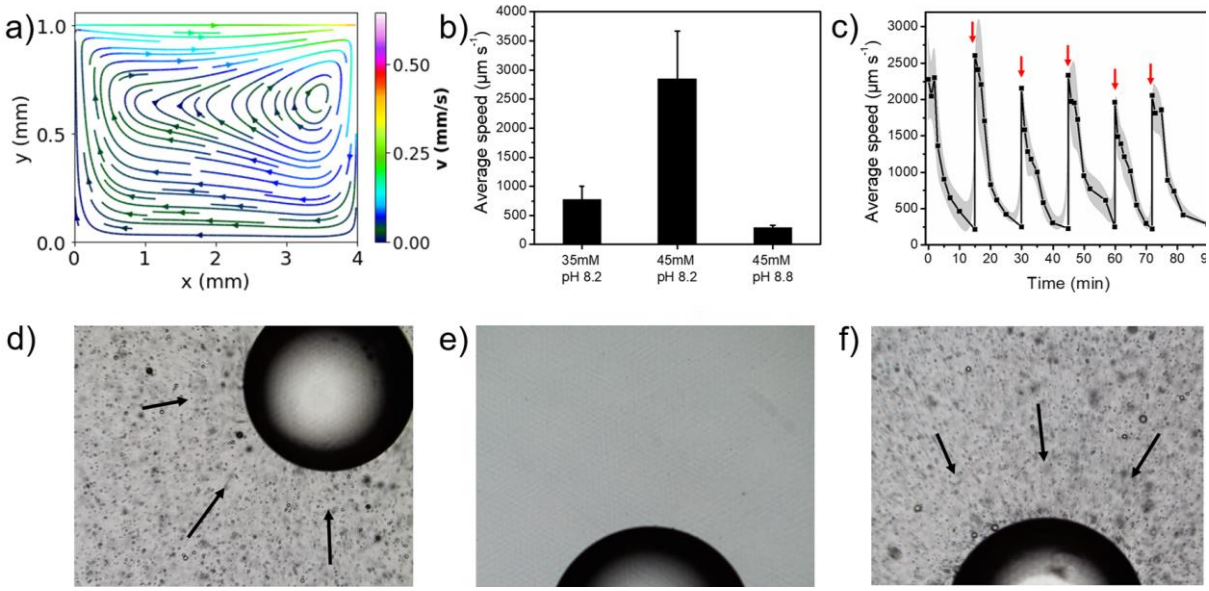

Figure 4. a) Stream plot of a simulated Marangoni flow in a cavity geometry. The color scale indicates the speed of the flow in mm s^{-1}. The system was modelled using a rate of amine formation of S = 0.1 s^{-1} and with a sequestration efficiency Γ_r = 0.5. For behavior at other values of S and Γ_r see Figure S20. b) Speed of motion averaged over 5 amide-based droplets prepared using different concentrations of **1a** or initial pH when approaching oleic acid. Error bars show the standard deviation. c) Time-dependence of the speed of motion of the droplets prepared using the same condition as Fig 3d. The arrows indicate the time points when EDC-HCl (60 mM) was added. Shaded areas show the standard deviation (n=5). Representative frames showing (d) the small amide-based droplets while they are moving towards the oleic acid droplet; (e) the same system after the amide-based droplets had dissolved, and (f) amide droplets after being regenerated by addition of EDC.

The hydrodynamic flow benefits from the presence of the amide-based droplets. As we showed above, EDC-fueled self-assembly can regenerate these droplets from spent reactants. Hence EDC should be able to fuel the Marangoni flow. As shown in Figure 4c and 4d, the amide droplets prepared from **2** (30 mM) and (**1a**, 45 mM) in an aqueous solution containing sodium borate (50 mM, pH 8.2) show motion for ~15 min after adding oleic acid (Video S10*,* Figure 4c), and the speed of movement decreased once the droplets had largely disintegrated (Figure 4e). We found that, upon regenerating the amide droplets by adding EDC-HCl, fast droplet movement occurred after adding oleic acid, as in the initial system (Figure 4c,f, Video S11). The EDC-fueled onset of motion was repeated another 4 times (see Video S12-15).

Conclusions

In summary, transient amide-based droplets were developed through the integration of a dissipative reaction cycle and self-assembly. The coacervate-like droplets were formed by co-assembly of starting amine and transient amide. The fact that the starting amine is liberated again upon amide hydrolysis gives rise to unusual dynamics: a double pulse of droplets arises from a single addition of reactants. These dynamic materials were used as a component in the design of a chemically fueled Marangoni flow system where the droplets fulfill the role of a surfactant-storing and releasing subsystem. Coupling it to a spatially localized sink for the same surfactant, in the form of a droplet of oleic acid on the sample surface, establishes a gradient of surfactant coverage of the air-water interface, giving rise to a gradient in surface tension. The latter drives a macroscopic Marangoni flow, which transports the amide droplets that are partially responsible for establishing this gradient. The system can be re-charged and flow re-started by addition of EDC which re-activates spent reagents.

This work couples molecular scale bond formation and breakage, via microscale dissipative self-assembled structures to macroscale fluid dynamics and provides a strategy to use dissipative chemistry for the design of chemical engines[51]. The rich dynamic behavior of droplet formation (double pulses), the ability of the droplets to promote their own formation, the ability to take up and release guest molecules, and induce motion, together with the surfactant components also makes this system a promising protocell model[52]. Finally, the underlying dynamic amide chemistry broadens the scope of dynamic covalent bonds that can be applied in dissipative systems chemistry[53,54].

References

1 Karsenti, E. Self-organization in cell biology: a brief history. *Nat. Rev. Mol. Cell Biol.* **9**, 255-262 (2008).

2 Walczak, C. E., Cai, S. & Khodjakov, A. Mechanisms of chromosome behaviour during mitosis. *Nat. Rev. Mol. Cell Biol.* **11**, 91-102 (2010).

3 Van Esch, J. H., Klajn, R. & Otto, S. Chemical systems out of equilibrium. *Chem. Soc. Rev.***46**, 5474-5475 (2017).

4 Fialkowski, M. *et al.* Principles and implementations of dissipative (dynamic) self-assembly. *J. Phys. Chem. B* **110**, 2482-2496 (2006).

5 Mattia, E. & Otto, S. Supramolecular systems chemistry. *Nat. Nanotechnol.* **10**, 111-119 (2015).

6 Heinen, L. & Walther, A. Celebrating Soft Matter's 10th Anniversary: Approaches to program the time domain of self-assemblies. *Soft Matter* **11**, 7857-7866 (2015).

7 van Rossum, S. A., Tena-Solsona, M., van Esch, J. H., Eelkema, R. & Boekhoven, J. Dissipative out-of-equilibrium assembly of man-made supramolecular materials. *Chem. Soc. Rev.* **46**, 5519-5535 (2017).

8 Ragazzon, G. & Prins, L. J. Energy consumption in chemical fuel-driven self-assembly. *Nat. Nanotechnol.* **13**, 882-889 (2018).

9 Weißenfels, M., Gemen, J. & Klajn, R. Dissipative self-assembly: Fueling with chemicals versus light. *Chem* **7**, 23-37 (2021).

10 Boekhoven, J., Hendriksen, W. E., Koper, G. J., Eelkema, R. & van Esch, J. H. Transient assembly of active materials fueled by a chemical reaction. *Science* **349**, 1075-1079 (2015).

11 Maiti, S., Fortunati, I., Ferrante, C., Scrimin, P. & Prins, L. J. Dissipative self-assembly of vesicular nanoreactors. *Nat. Chem.* **8**, 725-731 (2016).

12 Tena-Solsona, M. *et al.* Non-equilibrium dissipative supramolecular materials with a tunable lifetime. *Nat. Commun.* **8**, 1-8 (2017).

13 Kumar, M. *et al.* Amino-acid-encoded biocatalytic self-assembly enables the formation of transient conducting nanostructures. *Nat. Chem.* **10**, 696-703 (2018).
14 Bal, S., Ghosh, C., Ghosh, T., Vijayaraghavan, R. K. & Das, D. Non-Equilibrium Polymerization of Cross-β Amyloid Peptides for Temporal Control of Electronic Properties. *Angew. Chem.-Int. Edit.* **58**, 244-247 (2020).
15 Wang, S., Yue, L., Wulf, V., Lilienthal, S. & Willner, I. Dissipative Constitutional Dynamic Networks for Tunable Transient Responses and Catalytic Functions. *J. Am. Chem. Soc.* **142**, 17480-17488 (2020).
16 Che, H., Cao, S. & Van Hest, J. C. Feedback-induced temporal control of "breathing" polymersomes to create self-adaptive nanoreactors. *J. Am. Chem. Soc.* **140**, 5356-5359 (2018).
17 Donau, C. et al. Active coacervate droplets as a model for membraneless organelles and protocells. *Nat. Commun.* **11**, 1-10 (2020).
18 Späth, F. *et al.* Molecular Design of Chemically Fueled Peptide–Polyelectrolyte Coacervate-Based Assemblies. *J. Am. Chem. Soc.* **143**, 4782-4789 (2021).
19 Deng, J. & Walther, A. Programmable ATP-fueled DNA coacervates by transient liquid-liquid phase separation. *Chem* **6**, 3329-3343 (2020).
20 Giuseppone, N. & Walther, A. *Out-of-equilibrium (supra) molecular Systems and Materials*. (Wiley Online Library, 2021).
21 Das, K., Gabrielli, L. & Prins, L. J. Chemically Fueled Self-Assembly in Biology and Chemistry. *Angew. Chem.-Int. Edit.* **60**, 2-26, (2021).
22 Aprahamian, I. The future of molecular machines. *ACS Cent. Sci.* **6**, 347-358 (2020).
23 Te Brinke, E. *et al.* Dissipative adaptation in driven self-assembly leading to self-dividing fibrils. *Nat. Nanotechnol.* **13**, 849-855 (2018).
24 Cheng, G. & Perez-Mercader, J. Dissipative self-assembly of dynamic multicompartmentalized microsystems with light-responsive behaviors. *Chem* **6**, 1160-1171 (2020).
25 Leira-Iglesias, J., Tassoni, A., Adachi, T., Stich, M. & Hermans, T. M. Oscillations, travelling fronts and patterns in a supramolecular system. *Nat. Nanotechnol.* **13**, 1021-1027 (2018).
26 Hwang, I. *et al.* Audible sound-controlled spatiotemporal patterns in out-of-equilibrium systems. *Nat. Chem.* **12**, 808-813 (2020).
27 Kassem, S. *et al.* Artificial molecular motors. *Chem. Soc. Rev.* **46**, 2592-2621 (2017).
28 Oster, G. & Wang, H. Rotary protein motors. *Trends Cell Biol.* **13**, 114-121 (2003).
29 Needleman, D. & Dogic, Z. Active matter at the interface between materials science and cell biology. *Nat. Rev. Mater.* **2**, 1-14 (2017).
30 Sánchez, S., Soler, L. & Katuri, J. Chemically powered micro-and nanomotors. *Angew. Chem.-Int. Edit.* **54**, 1414-1444 (2015).
31 Velegol, D., Garg, A., Guha, R., Kar, A. & Kumar, M. Origins of concentration gradients for diffusiophoresis. *Soft matter* **12**, 4686-4703 (2016).
32 Chaudhury, M. K. & Whitesides, G. M. How to make water run uphill. *Science* **256**, 1539-1541 (1992).
33 Hanczyc, M. M., Toyota, T., Ikegami, T., Packard, N. & Sugawara, T. Fatty acid chemistry at the oil− water interface: Self-propelled oil droplets. *J. Am. Chem. Soc.* **129**, 9386-9391 (2007).

34 Babu, D. *et al.* Acceleration of lipid reproduction by emergence of microscopic motion. *Nat. Commun.* **12**, 1-7 (2021).

35 Nakata, S. & Murakami, M. Self-motion of a camphor disk on an aqueous phase depending on the alkyl chain length of sulfate surfactants. *Langmuir* **26**, 2414-2417 (2010).

36 Cejkova, J., Novak, M., Stepanek, F. & Hanczyc, M. M. Dynamics of chemotactic droplets in salt concentration gradients. *Langmuir* **30**, 11937-11944 (2014).

37 Varanakkottu, S. N. *et al.* Particle manipulation based on optically controlled free surface hydrodynamics. *Angew. Chem.-Int. Edit.***52**, 7291-7295 (2013).

38 Scriven, L. & Sternling, C. The marangoni effects. *Nature* **187**, 186-188 (1960).

39 Ikezoe, Y., Washino, G., Uemura, T., Kitagawa, S. & Matsui, H. Autonomous motors of a metal–organic framework powered by reorganization of self-assembled peptides at interfaces. *Nat. Mater.* **11**, 1081-1085 (2012).

40 Cheng, M. *et al.* Parallel and precise macroscopic supramolecular assembly through prolonged Marangoni motion. *Angew. Chem.-Int. Edit.* **57**, 14106-14110 (2018).

41 Nguindjel, A.-D. C. & Korevaar, P. A. Self-sustained Marangoni Flows Driven by Chemical Reactions. ChemSystemsChem **3**, 2021, e2100021.

42 Su, S., Du, F.-S. & Li, Z.-C. Synthesis and pH-dependent hydrolysis profiles of mono-and dialkyl substituted maleamic acids. *Org. Biomol. Chem.* **15**, 8384-8392 (2017).

43 Astoricchio, E., Alfano, C., Rajendran, L., Temussi, P. A. & Pastore, A. The wide world of coacervates: from the sea to neurodegeneration. *Trends Biochem. Sci.* **45**, 706-717 (2020).

44 Douliez, J. P. *et al.* Catanionic Coacervate Droplets as a Surfactant-Based Membrane-Free Protocell Model. *Angew. Chem.-Int. Edit.* **56**, 13689-13693, (2017)**.**

45 Walde, P., Wick, R., Fresta, M., Mangone, A. & Luisi, P. L. Autopoietic self-reproduction of fatty acid vesicles. *J. Am. Chem. Soc.* **116**, 11649-11654 (1994).

46 Bender, M. L., Chow, Y.-L. & Chloupek, F. Intramolecular Catalysis of Hydrolytic Reactions. II. The Hydrolysis of Phthalamic Acid. *J. Am. Chem. Soc.* **80**, 5380-5384 (1958).

47 Nakajima, N. & Ikada, Y. Mechanism of amide formation by carbodiimide for bioconjugation in aqueous media. *Bioconjugate Chem.* **6**, 123-130 (1995).

48 Meredith, C. H. et al. Predator–prey interactions between droplets driven by non-reciprocal oil exchange. *Nat. Chem.* **12**, 1136-1142 (2020).

49 Banerjee, A. & Squires, T. M. Long-range, selective, on-demand suspension interactions: Combining and triggering soluto-inertial beacons. *Sci. Adv.* **5**, eaax1893 (2019).

50 Chandrasekhar, S. *Hydrodynamic and hydromagnetic stability*. (Courier Corporation, 2013).

51 Amano, S., Borsley, S., Leigh, D. A. & Sun, Z. Chemical engines: driving systems away from equilibrium through catalyst reaction cycles. *Nat. Nanotechnol.* **16**, 1057-1067 (2021).

52 Martin, N. & Douliez, J. P. Fatty acid vesicles and coacervates as model prebiotic protocells. *ChemSystemsChem* **3**, e2100024 (2021).

53 Singh, N., Formon, G. J., De Piccoli, S. & Hermans, T. M. Devising synthetic reaction cycles for dissipative nonequilibrium self-assembly. *Adv. Mater.* **32**, 1906834 (2020).

54 Kariyawasam, L. S., Hossain, M. M. & Hartley, C. S. The transient covalent bond in abiotic nonequilibrium systems. *Angew. Chem.-Int. Edit.* **60**, 12648-12658 (2021).

Acknowledgements

The authors thank Nathalie Katsonis, Alexander Ryabchun, and Dhanya Babu for helpful discussion and Victor V. Krasnikov for performing the confocal experiments. This work was supported by the Dutch Ministry of Education, Culture and Science (Gravitation program 024.001.035), the oLife Cofund program, the ERC (AdG 741774) and a Marie Curie Individual Fellowship for K.L. (PSR 786350).

Contributions

S.O., K.L., and B.M. conceived and designed the project. K.L. performed experiments and analysed the data. A.B., S.D., and S.H. were responsible for the model. A.K. carried out the cryo-TEM experiments. All authors participated in the discussions. K.L. and S.O. wrote the paper.